Structural Characterization of Glycoconjugate Polystyrene in Aqueous Solution

Isao Wataoka,[†] Hiroshi Urakawa,[†] Kazukiyo Kobayashi,[‡] Toshihiro Akaike,[§] Manfred Schmidt,[||] and Kanji Kajiwara*[,†]

Faculty of Engineering & Design, Kyoto Institute of Technology, Kyoto, Sakyo-ku, Matsugasaki, 606-8585 Japan, Graduate School of Engineering, Nagoya University, Nagoya, Chikusa-ku, 464-8603 Japan, Faculty of Bioscience and Biotechnology, Tokyo Institute of Technology, Yokohama, Midori-ku, 227-8501 Japan, and Institut für physikalische Chemie, Johannes-Gutenberg-Universität Mainz, Mainz, Germany

Received June 9, 1998; Revised Manuscript Received January 4, 1999

ABSTRACT: Maltopentaose-carrying polystyrene was synthesized by the homopolymerization of vinylbenzyl maltopentaose amide. Resulted amphiphilc polymacromonomer was dissolved in 0.1 M urea aqueous solution, and its structure was characterized by small-angle X-ray scattering and molecular modeling. Maltopentaose-carrying polystyrene polymacromonomer was found to be represented by a molecular bottlebrush, composed of a large helix of polystyrene backbone and maltopentaose brushes. The molecular bottlebrush seems to be distributed randomly or many even be broken once or twice in segments with no apparent intersegmental spatial correlation. A large helix of polystyrene backbone is formed by a random sequence of TT, TG, and/or TTGG.

1. Introduction

Considerable attention has been paid for the design of biofunctional materials carrying the ligand on synthetic polymers.[1] Those novel materials are expected to be useful in biomedical systems such as cell separation, cell culture, drug delivery agent, and artificial antigen. Carbohydrate is one of the most important candidates to be a ligand or recognition signal. In this context, a convenient synthetic route[2] was developed to construct amphiphilic structures by arranging hydrophobic polystyrene main chains and hydrophilic pendant oligosaccharides. Synthesized glycoconjugate polymers (oligosaccharide carrying polystyrene derivatives) were found to function as highly sensitive ligands. Here highly concentrated multiantennary glyco signals along the hydrophobic main chains enhance the interaction with various types of carbohydrate-binding proteins. The enhancement is also attributed to the presence of the hydrophobic phenyl aglycon, although its active role is not clearly explained.[3] However, it is easily imagined that the activity depends on the chain conformation of a glycoconjugate polymer in water.

An oligosaccharide-carrying polystyrene derivative is classified as a polymacromonomer specified as a type of comb-shaped polymer possessing relatively long side chains with a regular interval. An extensive research effort has been focused to prepare densely grafted polymacromonomer by polymerizing a macromonomer, that is, a high molecular weight precursor (end-functionalized oligomer) for well-defined graft polymerization.[4−6] Despite the flexible nature of the main chains, polymacromonomers composed of poly(methyl methacrylate) or polystyrene backbone with oligostyrene side chains revealed an almost rigid rodlike conformation in solution[7−9] and a tendency to form a lyotropic mesophase.[10] The extended structure of main chains is apparently caused by the overcrowded oligopolystyrene side chains separated only by a contour distance of 2.5 Å, while the backbone and side chains are characterized by a random coil in the polymacromonomer having lower degrees of polymerization than 20.[9]

The present paper aims to characterize the conformation of amphiphilic polymacromonomer in aqueous solution by means of small-angle X-ray scattering. The maltopentaose-carrying polystyrene was chosen as a target polymer for this purpose. This polymacromonomer in aqueous solution shows a different ability for molecular recognition from that on the plastic plate,[11] and the cause of this difference is speculated as being due to the change of the conformation of this glycoconjugate polymer.

2. Experimental Section

Vinylbenzyl maltopentaose amide (VM5A) was synthesized from maltopentaose lactone by coupling with *p*-vinylbenzylamine as described elsewhere.[12] The radical homopolymerization of VM5A yields maltopentaose-carrying polystyrene (coded as PVM5A), which is soluble in water, dimethylformamide (DMF) and dimethyl sulfoxide (Me_2SO). See Scheme 1.

Small-angle X-ray scattering (SAXS) was observed from 0.1 M urea aqueous solutions of PVM5A. The measurement was performed with an SAXES[13] (small-angle X-ray scattering equipment for solutions) installed at the BL-10C of the Photon Factory, Tsukuba, Japan. An incident X-ray from synchrotron radiation was monochromatized to $\lambda = 1.488$ Å and then focused to the position of the detector with a bent mirror. The scattered X-ray was detected by the one-dimensional position sensitive proportional counter (PSPC) of the effective length, 160 mm. The exact camera length was calibrated by using the diffraction peaks of collagen fiber (the long period = 670 Å at the sixth, ninth, and 11th orders). The scattered X-ray was accumulated to the total measuring time of 30 min

* Corresponding author.
[†] Kyoto Institute of Technology.
[‡] Nagoya University.
[§] Tokyo Institute of Technology.
[||] Johannes-Gutenberg-Universität Mainz.

10.1021/ma9809132 CCC: $18.00
Published on Web 03/05/1999

Scheme 1. Maltopentaose-Carrying Styrene Macromonomer (VM5A) and Its Homopolymerization to Maltopentaose-Carrying Polystyrene (PVM5A)

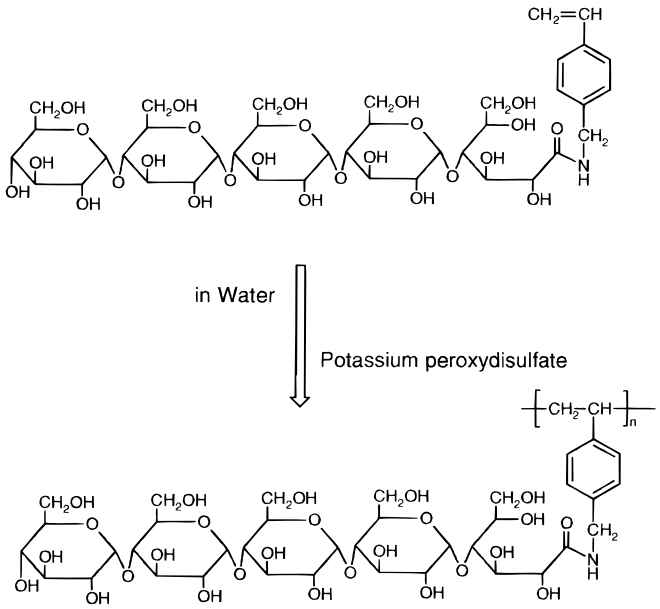

in order to have a sufficient signal-to-noise ratio. The sample solutions were prepared by weighing polymacromonomer directly in the sample bottle and adding solvent to adjust the concentration of the solutions. The solutions were injected into the flat cells (1 cm × 0.5 cm × 0.1 cm) fitted with a pair of thin quartz windows (20 μm in thickness). Respective cells were mounted in the cell holder aligned in the SAXES, and the solution temperature was maintained at 25 °C by circulating water of a constant temperature through the cell holder. The scattered intensities were corrected for the variation of the incident X-ray flux by monitoring the beam with an ionizing chamber placed in front of the sample holder. The excess scattering intensities were evaluated by subtracting the scattering intensities of solvent from those of polymacromonomer solutions.

Dynamic and static light scattering was observed from PVM5A in 0.1 M urea aqueous solutions with an ALV SP-86 goniometer equipped with either an ALV-3000 correlator and Kr-ion laser (647.1 nm wavelength, 500 mW) or an ALV-5000 correlator and Nd:YAG laser (532,0 nm, 80 mW). Recorded correlation functions were analyzed by the cumulants method.

The molecular model was generated with the program Cerius 2 ver 2 (BIOSYM/Molecular Simulations) on a Silicon Graphics O_2 workstation. The universal force field 1.01[14] was used for energy minimization and molecular dynamics. The molecular mechanics minimization was performed at first on the molecular model constructed artificially. The resulting model by molecular mechanics minimization was annealed by affording a thermal disturbance and then was energy-minimized the second time by molecular mechanics. Energy minimization was achieved in the system containing solvent by the use of a conjugate gradient algorithm until the root-mean-square force became less than 0.10 kcal/(mol·Å) or the number of the minimization step exceeded 3000 in the case of the initial minimization. The molecular dynamics simulation was performed for annealing at a constant volume under conditions identical with those described for the energy minimization by the molecular mechanics. The temperature of the system was initially fixed at 300 K, increased to 500 K, and then cooled to 300 K with a temperature increment or decrement of 50 K. One cycle consists of 50 steps at each temperature from 300 to 500 K and then down to 350 K, and the elapsed time for 1 step corresponds to 0.0010 ps. Thus the total simulation time amounts to 2.05 ps.

The particle scattering factor is calculated from the atomic coordinates of each generated molecular model according to

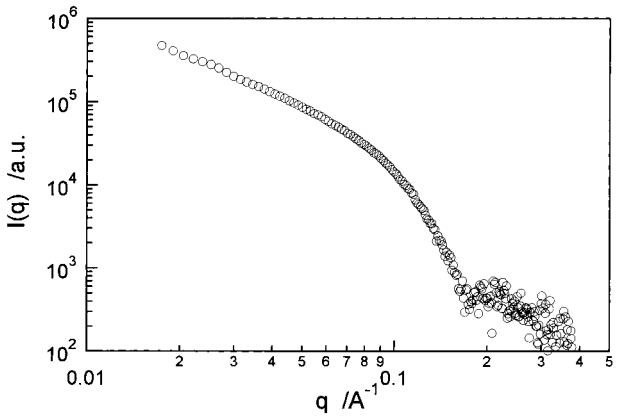

Figure 1. Double logarithmic plots of the small-angle X-ray scattering results from PVM5A in 0.1 M urea aqueous solution.

the Debye formula, so that the scattering profile is given by

$$I(q) \approx \sum_{i=1}^{n} g_i^2 \phi_i^2(q) + 2\sum_{i=1}^{n-1} \sum_{j=i+1}^{n} g_i g_j \phi_i(q) \phi_j(q) \frac{\sin d_{ij}q}{d_{ij}q} \quad (1)$$

where q denotes the magnitude of a scattering vector given by $(4\pi/\lambda)\sin\theta$ with θ and λ being half of the scattering angle and the wavelength of an incident X-ray, respectively. g_i is an atomic scattering factor, and d_{ij} is the distance between the ith and the jth atoms. The form factor for the ith atom, $\phi_i(q)$, is assumed to be given by the form factor of a sphere having a radius equivalent to a van der Waals radius of the ith atom as

$$\phi_i^2(q) = \frac{3[\sin(R_i q) - (R_i q)\cos(R_i q)]}{(R_i q)^3} \quad (2)$$

with R_i being the van der Waals radius of the ith atom.

3. Results and Discussion

Figure 1 shows the small-angle X-ray scattering (SAXS) profile from PVM5A in 0.1 M urea aqueous solution in the double-logarithmic plots. The SAXS profile is characterized by a minimum at about $q = 0.18$ Å^{-1}.

The radius of gyration R_g and the degree of polymerization D_p were evaluated as 214 Å and 650 (equivalent to 6.4×10^5 in terms of the weight average molecular weight M_w), respectively, for PVM5A by light scattering. The light scattering measurement was carried out on polymacromonomer in 0.1 M urea aqueous solution of PVM5A in order to prevent aggregation by intermolecular hydrogen bonding.

When a molecule is rodlike, the scattering from such a molecule is approximately given in terms of the cross-sectional radius of gyration R_{gc} as[15]

$$qI(q) \approx \exp\left(-\frac{q^2 R_{gc}^2}{2}\right) \quad (3)$$

The relationship (the Guinier approximation for a cross-section) holds in the range where $qR_g \geq 1$ and $qR_{gc} \leq 1$, and R_{gc} is determined from the slope of ln $qI(q)$ plotted against q^2 (referred to as the cross-sectional Guinier plots) in an appropriate range of q. The example of the cross-sectional Guinier plots is shown in Figure 2. The plots confirm a good linearity expected from eq 3 in an appropriate range of q, and the value of $R_{gc} = 17.3$ Å

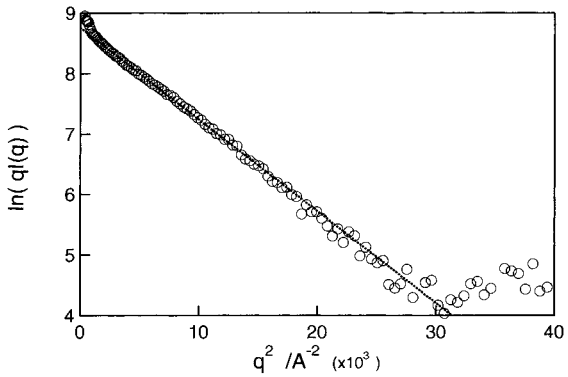

Figure 2. Cross-sectional Guinier plots for PVM5A, where a solid line represents the Guinier approximation for cross-section (eq 3).

was evaluated from the slope in Figure 2. Since R_g of a rodlike molecule follows the relationship

$$R_g^2 = R_{gc}^2 + \frac{h^2}{12} \tag{4}$$

where h denotes the length of a rodlike molecule, eq 4 allows evaluating the rod length as $h = 740$ Å from the values of R_g and R_{gc} evaluated as above from the results of light scattering and SAXS, respectively.

The hydrodynamic radius R_H of PVM5A was evaluated as 148 Å in 0.1 M urea aqueous solution by dynamic light scattering. Here the bimodal distribution of the correlation function was observed, suggesting the existence of a small amount of aggregates. Since the hydrodynamic radius R_H of a cylinder is given in terms of the length h and the hydrodynamically effective cross-sectional diameter d_H by[16]

$$R_H = \frac{h}{[2 \ln(h/d_H)]} \tag{5}$$

As $h = 740$ Å and $R_H = 148$ Å as estimated from the static/dynamic light and small-angle X-ray scattering, the hydrodynamically effective cross-sectional diameter d_H is calculated from eq 5 as 60.7 Å. The cross-sectional diameter d is calculated from the cross-sectional radius of gyration as

$$d = \sqrt{8} R_{gc} \tag{6}$$

by assuming a constant electron density across the cylinder. Equation 6 yields $d = 48.9$ Å, which is smaller than the hydrodynamically effective cross-sectional diameter. Although small errors in R_H results in a large uncertainty in the d_H value and a cylindrical shape is a priori assumed, the larger hydrodynamically effective cross-sectional diameter may indicate the hydration due to maltopentaose side chains. A similar tendency was observed for polymacromonomers of poly(methyl methacrylate) backbone with oligostyrene side chains.[8]

The rod length per monomer unit corresponds to 1.14 Å in PVM5A, while a much larger value (2.5−3.1 Å) was found for the polymacromonomer consisting of polymethyl methacrylate backbone with oligostyrene side chains.[8] This short rod length per monomer suggests the shrunken backbone for PVM5A in comparison with that of poly(methyl methacrylate). The main chain is rather extended to accommodate overcrowded side chains in the polymacromonomer consisting of poly(methyl methacrylate) and oligostyrene, whereas the main chain of PVM5A should assume a large helical conformation to account for a short rod length per monomer. Hydrophilic side chains would cover a hydrophobic main chain of PVM5A so as not to contact the main chain directly with water.

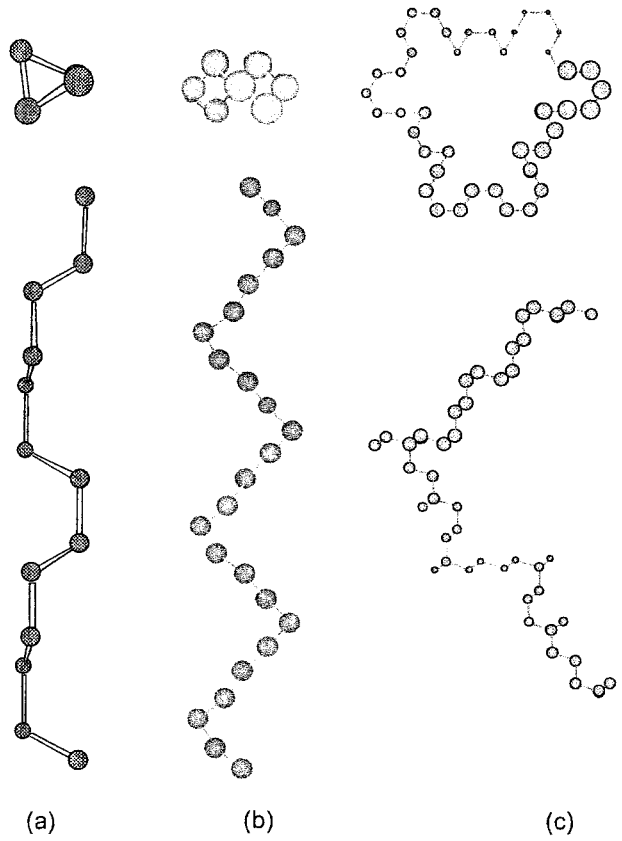

Figure 3. The main chain conformation adopted for the molecular model of maltopentaose-carrying polystyrene: (a) a TG helix; (b) a TTGG helix; (c) a large helix composed of a random sequence of TT, TG, and/or TTGG.

To clarify this situation, the molecular models representing PVM5A were constructed by Cerius2 as follows, and the particle scattering factor calculated from each generated chain was compared with the observed SAXS profile. Isotactic polystyrene assumes the regular TG (trans−gauche) conformation, while syndiotactic polystyrene has TT (trans−trans) or TTGG (trans−trans−gauche−gauche) conformations in respective crystalline phase.[17] Since PVM5A is considered to be atactic, the helix of PVM5A, if formed, may consist of the random sequence of TG, TT, and/or TTGG.

Parts a and b of Figure 3 show the main chain conformations composed of TG and TTGG sequence, respectively, and the corresponding particle scattering factors were calculated from eq 1 as shown in Figure 4. Although the observed scattering profile shows a minimum at $q = 0.175$ Å^{-1}, the scattering profile calculated from the molecular model composed of the TTGG sequence or the TG sequence has no minimum or a minimum at $q = 0.195$ Å^{-1}, respectively. Here the degree of polymerization D_p of the models is fixed to 96 because no appreciable change is observed in the calculated scattering profile in the q range accessed experimentally when D_p exceeds 96 in the case of the TG or TTGG sequence. The cross-sectional radius of gyration was evaluated for those models as 13.1 Å

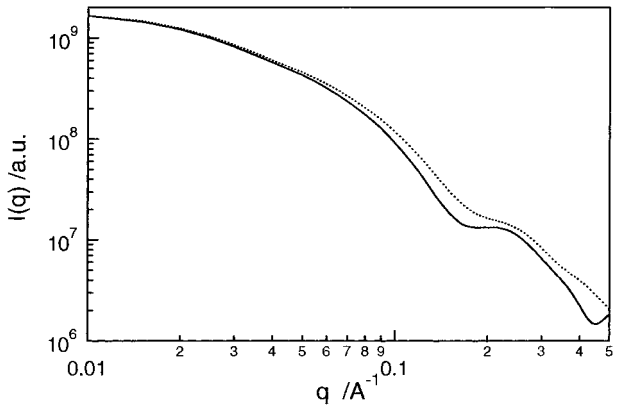

Figure 4. Scattering profiles calculated from two molecular models of maltopentaose-carrying polystyrene (D_p = 324), constructed from a TG polystyrene helix (a solid line) and a TTGG polystyrene helix (a broken line).

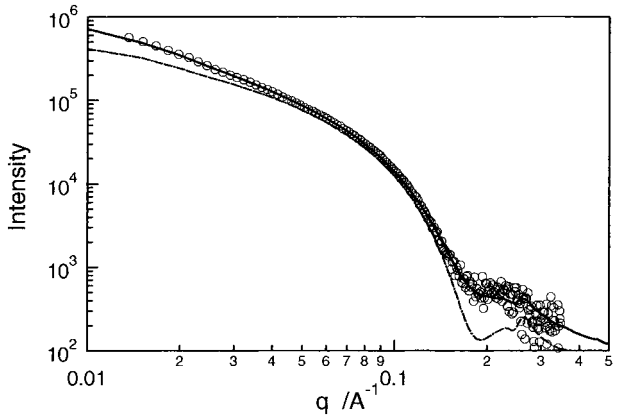

Figure 5. Scattering profile calculated from the maltopentaose-carrying polystyrene model, constructed from a large polystyrene helix. A one-dot broken line represents the calculated profile directly from the molecular model (D_p = 324), and a solid line is calculated by taking into account the effect of aggregation and backbone-folding. Open circles show the observed SAXS profile from PVM5A.

(TTGG) or 14.8 Å (TG), which is considerably smaller than the value of 17.3 Å evaluated for PVM5A experimentally. Thus PVM5A should form a larger helix composed of random sequences of TT, TG, and TTGG in order to account for the rodlike shape with a large cross-section and the hydrophilic nature of the molecular surface. A large helix model was built by the random sequence of TT, TG, and TTGG as shown in Figure 3c, which yields the cross-sectional radius of gyration as 17.4 Å. The particle scattering factor calculated from this model (D_p = 324) is shown by a one-dot broken line in Figure 5.

Despite of the correct value of the cross-sectional radius, two major discrepancies will be observed at high and low q ranges, when compared the calculated scattering profile with the SAXS profile of PVM5A. The fine structure around q = 0.17−0.3 Å^{-1} observed in the calculated scattering profile is less distinct in the SAXS profile of PVM5A. This may suggest that a local structure is not so clearly specified as in the molecular model and a regular helical conformation is broken in parts. In fact, the broken rod structure was observed from the polymacromonomer composed of poly(methyl methacrylate) backbone with oligostyrene side chains by a scanning force microscopy (SFM).[18,19] Thus it would be appropriate to adopt the modified broken rod

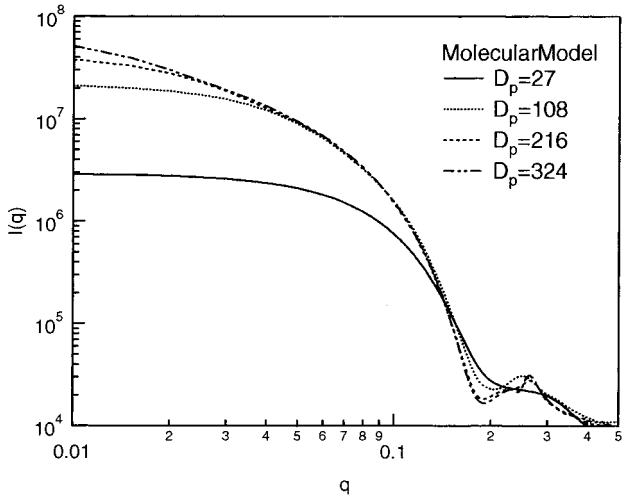

Figure 6. Calculated SAXS profile of the molecule model with different D_p.

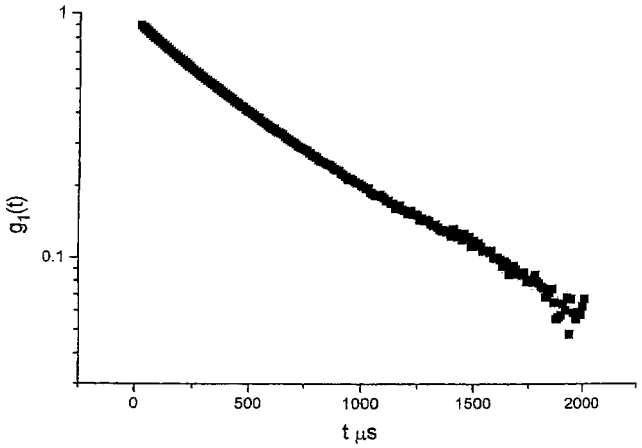

Figure 7. Time correration function measured in the dynamic light scattering.

model[19,20] for a further analysis. The scattering from the modified broken rod model is expressed as[20,21]

$$q^2 I(q)/c \approx \sum_i w_i M_{1i} \theta_i(q) + \text{constant} \qquad (7)$$

Here the subscript i denotes the ith component specified by the linear mass M_{1i} and the particle scattering factor $\Theta_i(q)$. The particle scattering factor $\Theta_i(q)$ is calculated according to eq 1 once a suitable molecular model has been constructed. The constant term in eq 7 accounts for the spatial correlation between the components being random.[22] That is, eq 7 implies that rod like pieces an distributed randomly in the ssystem and are not necessarily linked together. A single component of a large helix Figure 3c will be considered in the present analysis.

To evaluate the influence of the rod length on the scattering profile, the scattering profiles were calculated from the molecular models with the different degrees of polymerization (D_p) are shown in Figure 6. No D_p dependence was observed in large q range. The results indicates that the characteristic scattering profile at q = 0.17−0.3 Å^{-1} reflects the local structure and is not affected by the whole molecule. The deviation at a low q range from the calculated scattering profile is considered to be due to the existence of a small amount of aggregates observed in the dynamic light scattering

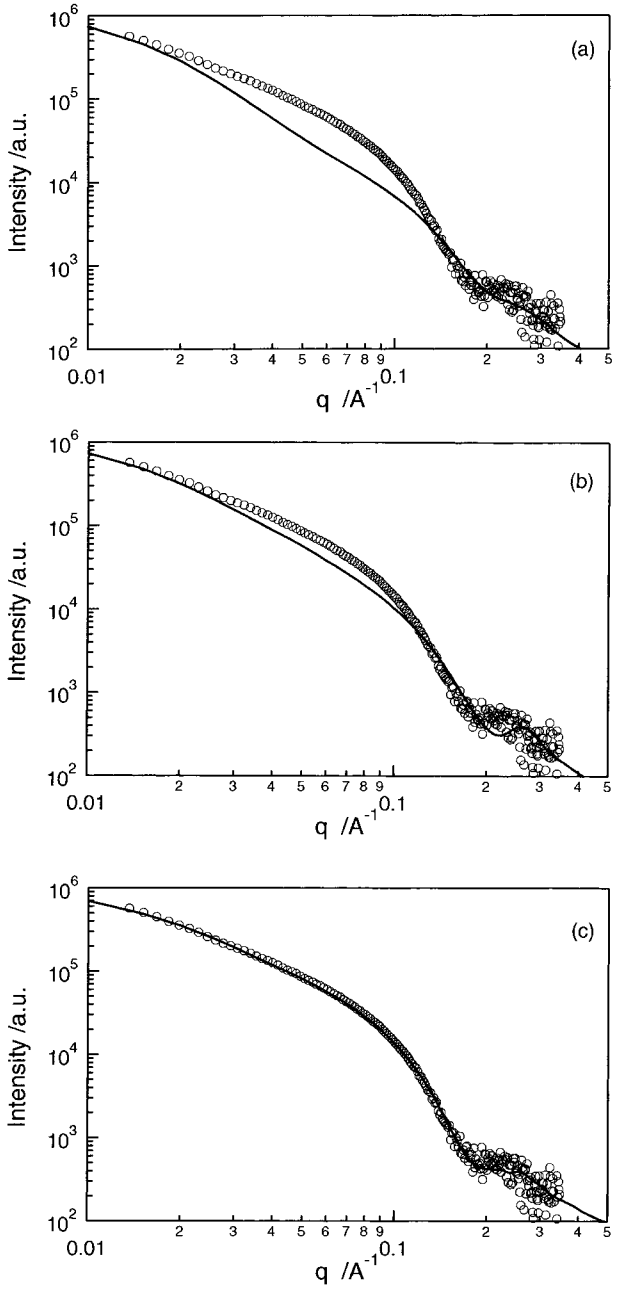

Figure 8. D_p dependence of the scattering profile from maltopentaose-carrying polystyrene, where the effect of aggregation is taken into account. Open circles show the observed SAXS profile from PVM5A. Key: (a) $D_p = 27$; (b) $D_p = 108$; (c) $D_p = 216$.

(Figure 7). The aggregates may be characterized by an inhomogeneous solidlike structure, and the scattering $I_{\text{Debye-Bueche}}(q)$ from such an aggregate is given by the Debye−Bueche function in terms of the extent of an inhomogeneity a as[23]

$$I_{\text{Debye-Buech}}(q) \cong \frac{a^3}{(1 + a^2q^2)^2} \tag{8}$$

so that the total scattering will be expressed by the sum of two scattering functions eqs 7 and 8. A solid line in Figure 5 is calculated from the sum of eqs 7 and 8, where $a = 50$ Å and $D_p = 324$. The fitting result with the observed SAXS profile is satisfactory and confirms that maltopentaose-carrying polystyrene has a cylindrical shape in water with a backbone chain

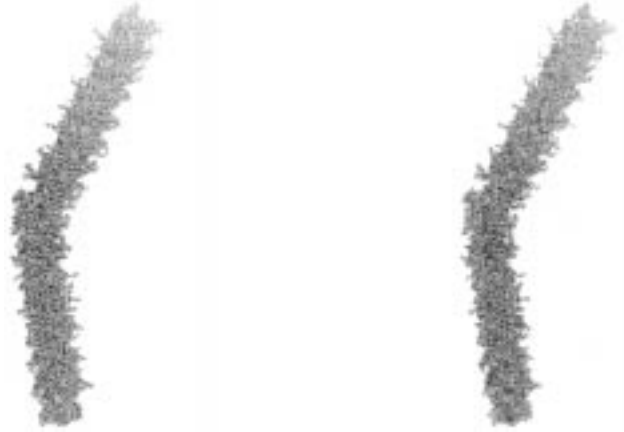

Figure 9. Molecular model of maltopentaose-carrying polystyrene (a stereoview).

assuming a large helical conformation. Here the cylinder are randomly distributed in a space, including the relatively short cylinders and the cylinders broken in parts.

A remaining task is to estimate the length of a cylindrical part. Although the present analysis will not allow evaluating the rod length directly, the D_p dependence of the scattering profile might provide an idea for the length of a cylindrical part. Figure 8 shows the calculated scattering profiles as a function of the degree of polymerization D_p. Here the particle scattering factor $\Theta_i(q)$ was calculated from the large helix model with varying D_p. according to the modified broken rod model (eq 7) and compared with the observed SAXS profile from PVM5A. Here the effect of larger aggregates is also incorporated by considering the Debye-Bueche term (eq 8). The fitting result becomes satisfactory when D_p exceeds approximately 200. Since no other criterion is available to estimate the length of cylindrical part, it can be concluded that the maltopentaose-carrying polystyrene is represented by a once- or twice-broken cylinder (see Figure 9), where the continuous length of a cylindrical part is at least 200 in terms of the degree of polymerization (equivalent to 230 Å). Shorter cylinders could also be present in the system, considering a broad molecular weight distribution of the sample. This model presents a figure consistent with the SFM observation[18,19] on the poly(methyl methacrylate) polymacromonomer with oligostyrene side chains.

4. Conclusion

Maltopentaose-carrying polystyrene polymacromonomer is characterized in the shape of a molecular bottlebrush in 0.1 M urea aqueous solution. The molecular bottlebrush is composed of a large helix of polystyrene backbone and maltopentaose brushes. The molecular bottlebrush seems to be broken once or twice in segments with no apparent intersegmental spatial correlation. A large helix of polystyrene is formed by a random sequence of TT, TG, and/or TTGG.

Acknowledgment. This work was performed under the approval of the Photon Factory Advisory Committee (Proposal No. 94G293, 97G139). We acknowledge financial support from a Grant-in-Aid for Scientific Research on Priority Areas from the Ministry of Education and Culture, Japan.

References and Notes

(1) Kobayashi, K.; Kobayashi, A.; Akaike, T. *Methods Enzymol.* **1994**, *247*, 409−418.
(2) Kobayashi, K.; Sumitomo, H.; Ina, Y. *Polym. J.* **1985**, *17*, 567−575.
(3) Kobayashi, K.; Tsuchida, A.; Usui, T.; Akaike, T. *Macromolecules* **1997**, *30*, 2016−2020.
(4) Chaumont, P.; Herz, J.; Remppe, P. *Eur. Polym. J.* **1979**, *15*, 459.
(5) Yamashita, Y. *J. Appl. Polym. Sci., Appl. Polym. Symp.* **1981**, *36*, 193.
(6) Schulz, G. O.; Milkovich, R. *J. Polym. Sci., Polym. Chem. Ed.*, **1984**, *22*, 1633−1652.
(7) Wintermantel, M.; Schmidt, M.; Tsukahara, Y.; Kajiwara, K.; Kohjiya, S. *Macromol. Chem. Rapid Commun.* **1994**, *15*, 279.
(8) Wintermantel, M.; Gerle, M.; Fischer, K.; Schmidt, M.; Wataoka, I.; Urakawa, H.; Kajiwara, K.; Tsukahara, Y. *Macromolecules* **1996**, *34*, 978.
(9) Wataoka, I.; Urakawa, H.; Kajiwara, K.; Schmidt, M.; Wintermantel, M. *Polym. Int.* **1997**, *44*, 365−370.
(10) Wintermantel, M.; Fischer, K.; Gerle, M.; Ries, R.; Schmidt, M. Kajiwara, K.; Urakawa, H.; Wataoka, I. *Angw. Chem. Int. Ed. Engl.* **1995**, *34*, 1472−1474.
(11) Matsuura, K.; Tsuchida, K.; Kobayashi, K.; Okahata, Y.; Akaike, T. *Macromolecules*, in press.
(12) Kobayashi, K.; Sumitomo, H.; Itoigawa, T. *Macromolecules* **1987**, *20*, 906.
(13) Ueki, T.; Hiragi, Y.; Izumi, Y.; Kataoka, M.; Muroga, Y.; Matsushita, T.; Amemiya, Y. *Photon Factory Activity Rep.* **1983**, *1*, V5, V29, V170.
(14) Rappe, A. K.; Casewit, C. J.; Coldwell, K. S.; Goddard, W. A.; Skiff, W. M. *J. Am. Chem. Soc.* **1992**, *114*, 10024.
(15) See, for example: Glatter, O., Kratky O., Eds. *Small-Angle X-ray Scattering*; Academic Press: London, 1982.
(16) See, for example: Yamakawa, H.; *Modern Theory of Polymer Solutions*; Harper & Row: New York, 1971.
(17) Kobayashi, M.; Nakaoki, T.; Ishihara, N. *Macromolecules* **1990**, *23*, 78.
(18) Dziezok, P.; Sheiko, S. S.; Fischer, K.; Schmidt, M.; Möller, M. *Angew. Chem., Int. Ed. Engl.* **1997**, *36*, 2812.
(19) Sheiko, S. S.; Gerle, M.; Fischer, K.; Schmidt, M.; Möller, M. *Langmuir* **1997**, *13*, 5368.
(20) Guenet, J.-M. *Thermoreversible Gelation of Polymers and Biopolymer*; Academic Press: London, 1992.
(21) Coviello, T.; Maeda, H.; Yuguchi, Y.; Urakawa, H.; Kajiwara, K.; Dentini, M.; Crescenzi, V. *Macromolecules* **1998**, *31*, 1602.
(22) Luzzati, V.: Benoit, H. *J. Apply. Crystallogr.* **1961**, *14*, 297.
(23) Debye, P.; Bueche, A. M. *J. Appl. Phys.* **1949**, *20*, 518.

MA9809132